Doping effects on the stability and superconductivity of penta-graphene-like ZrH_{10} and HfH_{10} under pressure

Hulei Yu[1] and Yue Chen[1,2,*]

[1] *Department of Mechanical Engineering, The University of Hong Kong, Pokfulam Road, Hong Kong SAR, China*
[2] *HKU Zhejiang Institute of Research and Innovation, 1623 Dayuan Road, Lin An 311305, China*

(Dated: July 18, 2022)

The discovery of room-temperature superconductors has aroused great attention in pressure-induced superhydrides. Herein, we explore the doping effects on the newly-proposed penta-graphene-like hydrides ZrH_{10} and HfH_{10} from first-principles calculations. Imaginary phonon frequencies of $P6_3/mmc$ ZrH_{10} and HfH_{10} at lower pressures are found to be eliminated by hole doping, leading to more accessible superconductivity. At high pressures, phonons are prone to be softened by electron doping, which increases the electron-phonon coupling and the superconducting critical temperature (T_c). Doping is found to be an effective way to lower the stabilization pressure and increase the T_c of $P6_3/mmc$ ZrH_{10} and HfH_{10}. This work paves an avenue for realizing low-pressure high-T_c superconducting hydrides.

Over the past few decades, the exploration of new superconductors with extraordinary superconductivity has attracted great scientific interest[1,2]. Due to the high vibrational frequencies and strong electron-phonon coupling (EPC), metallic hydrogen is expected to exhibit room-temperature superconductivity above a hydrostatic pressure of 400 GPa[3,4]. However, the ultra-high metallization pressure of pure hydrogen hinders further experimental study[4]. Hydrogen-dominant compounds, thus, become the most promising materials to achieve high superconducting critical temperatures (T_c) at relatively lower pressures[5–7].

Potential pressure-stabilized superhydrides with different hydrogen configurations have been predicted in various binary systems, and some of them have been experimentally synthesized. The first superhydride with a T_c over the record of cuprates (164 K at 31 GPa[8]), CaH_6, was reported by Wang et al. after systematically investigating the Ca-H binary system[9]. This clathrate CaH_6 was predicted to exhibit superconductivity below 200 K at 150 GPa[9,10], which was supported by recent experimental observation of superconductivity at 215 K in calcium superhydrides[11]. Following the idea of three dimensional (3D) clathrate hydrogen framework to support strong electron-phonon interaction[12], more clathrate-like superhydrides, including YH_6[13–15], CeH_9[16], ThH_{10}[17], YH_{10}[18], and LaH_{10}[18–20], were proposed and synthesized with near room temperature T_c under high pressures. Unlike 3D hydrogen motifs, a novel candidate of high-T_c superhydrides was proposed recently with a planar penta-graphene-like hydrogen sublattice. Such two dimensional (2D) layered structure can be stabilized in ZrH_{10} (T_c = 220 K at 250 GPa) and HfH_{10} (T_c = 234 K at 250 GPa) with large density of states (DOS) at Fermi level (E_F) and strong EPC[21,22]. In the sulfur-hydrogen system, compressed H_3S with isolated atomic hydrogen was experimentally observed to be superconducting at 203 K under a pressure of 155 GPa[23,24]. Recent experiments also confirmed that the carbonaceous sulfur hydride is a room-temperature superconductor[25].

Hole or electron doping has been proved to be an effective method to modify the superconductivity in unconventional superconductors[26–28]. However, the underlying mechanisms induced by doping in unconventional superconductors are elusive[29]. As conventional superconductors are driven by EPC, the doping effects on the superconductivity of hydrides can be relatively well understood based on the Bardeen-Cooper-Schrieffer theory[29,30]. Benefiting from extra electrons of Li dopant[31], the highest predicted T_c was reported by Sun et al. in electron-doped MgH_{16} under pressures[32]. Hole doping was applied to increase DOS by shifting E_F toward the symmetry-driven van Hove singularity, significantly enlarging T_c of clathrate CeH_9 under pressures[33]. Moreover, the outstanding superconductivity in carbonaceous sulfur hydride was also believed to be induced by hole doping[34].

Herein, we explore doping effects on the newly-proposed 2D penta-graphene-like ZrH_{10} and HfH_{10} under hydrostatic pressures. Both hole and electron dopings are found to play important roles in the lattice dynamical stability and superconductivity under pressures. Phonon properties with different doping conditions under pressures are systematically studied. It is found that the stabilization pressure ranges of ZrH_{10} and HfH_{10} can be effectively manipulated through hole doping, maintaining outstanding superconductivity at lower pressures. DOS and electron-phonon interactions are also calculated. The EPC of ZrH_{10} and HfH_{10} is found to become stronger under suitable electron doping at high pressures, leading to an enhanced T_c.

As implemented in Quantum Espresso[35,36], structural relaxations and electronic property calculations of ZrH_{10} and HfH_{10} were performed within the framework of density functional theory (DFT)[37], while lattice dynamics and EPC properties were explored within the density functional perturbation theory (DFPT)[38]. The interaction between ions and electrons was treated with the optimized norm-conserving Vanderbilt pseudopotential[39,40] in the generalized gradient approximation (GGA) ap-

plying the Perdew-Burke-Ernzerhof (PBE) functional[41]. Projector augmented wave (PAW)[42] type pseudopotentials were used to perform Bader charge analysis[43]. All calculations were performed with an energy cutoff of 90 Ry for the plane-wave basis, and the Gaussian broadening was set to 0.02 Ry. A dense Monkhorst-Pack k-grid of $24\times24\times36$ was utilized with a $4\times4\times6$ q-point mesh for the phonon and EPC calculations[44]. The EPC strength at wavevector q of mode υ is defined as

$$\lambda_{q\upsilon} = \frac{\gamma_{q\upsilon}}{\pi\hbar N(E_F)\omega^2} \tag{1}$$

where $\gamma_{q\upsilon}$, $\hbar$, $N(E_F)$, and ω are the phonon linewidth, the reduced Planck constant, DOS at E_F, and the phonon frequency, respectively. Given the Eliashberg spectral function $\alpha^2F(\omega)$, the averaged phonon frequency ω_{log} and the total EPC parameter λ can be determined:

$$\omega_{log} = exp[\frac{2}{\lambda}\int_0^\infty \frac{d\omega}{\omega}\alpha^2F(\omega)log\omega], \tag{2}$$

$$\lambda = 2\int_0^\infty \frac{\alpha^2F(\omega)}{\omega}d\omega \tag{3}$$

The Allen-Dynes (A-D) modified McMillan equation[45] was used to evaluate T_c with a typical value of the Coulomb pseudopotential μ^* (0.1-0.13):

$$T_c = f_1f_2\frac{\omega_{log}}{1.2}exp[\frac{-1.04(1+\lambda)}{\lambda-\mu^*(1+0.62\lambda)}] \tag{4}$$

where f_1 is the strong coupling correction factor, and f_2 is the shape correction factor. For $\lambda \leq 1.5$, f_1f_2 equals to 1, and for $\lambda > 1.5$,

$$f_1 = \sqrt[3]{[1+(\frac{\lambda}{2.46+9.348\mu^*})^{\frac{3}{2}}]}, \tag{5}$$

$$f_2 = 1+\frac{(\frac{\bar{\omega}}{\omega_{log}}-1)\lambda^2}{\lambda^2+[(1.82+11.466\mu^*)\frac{\bar{\omega}}{\omega_{log}}]^2}, \tag{6}$$

$$\bar{\omega} = \sqrt{\frac{2}{\lambda}\int_0^\infty \alpha^2F(\omega)\omega d\omega} \tag{7}$$

Due to the broad region of phonon spetrum of hydrides, Gor'kov and Kresin (G-K) developed another analytical expression for T_c by dividing the phonon spectrum into optical and acoustic parts[46]. According to Eq. 3 and Eq. 7, two EPC constants λ_a and λ_o, as well as the corresponding average frequencies $\bar{\omega}_a$ and $\bar{\omega}_o$ were introduced for acoustic and optical intervals, respectively. For ZrH_{10} and HfH_{10}, $\lambda_a << \lambda_o$; therefore,

$$T_c = [1+2\frac{\lambda_a}{\lambda_o-\mu^*}\frac{\omega_a^2}{(\pi T_c^o)^2+\omega_a^2}], \tag{8}$$

When $\lambda_o \leq 1.5$, T_c^o can be defined from Eq. 4:

$$T_c^o = \frac{\bar{\omega}_o}{1.2}exp[\frac{-1.04(1+\lambda_o)}{\lambda_o-\mu^*(1+0.62\lambda_o)}] \tag{9}$$

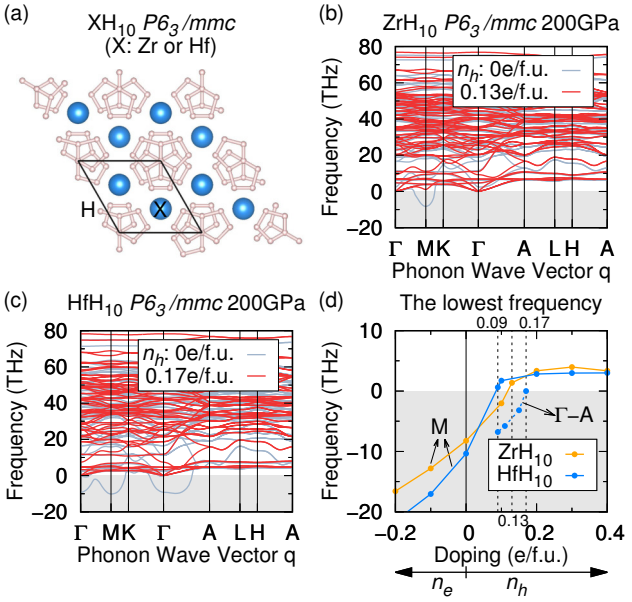

FIG. 1. (a) Crystal structure of $P6_3/mmc$ XH_{10}. Large blue spheres represent Zr or Hf atoms, and pink spheres denote H atoms. Phonon dispersions of pristine and doped ZrH_{10} (b) and HfH_{10} (c) at 200 GPa. (d) The lowest phonon frequency at M point and along Γ-A as a function of doping concentration at 200 GPa.

When $\lambda_o > 1.5$,

$$T_c^o = \frac{0.25\bar{\omega}_o}{[e^{\frac{2+4\mu^*+3\lambda_o\mu^*exp(-0.28\lambda_o)}{\lambda_o-\mu^*}}-1]^{0.5}} \tag{10}$$

The calculated superconductivities of the $P6_3/mmc$ phases at 300 GPa are in well agreement with previous studies[21] (see TABLE S1 in the Supporting Information).

Charge doping was realized by adding/removing the total number of electrons in the unit cell with a compensating uniform charge background of opposite sign for charge neutrality. This approach has been widely used in exploring the superconductivity of doped hydrides[29,33,47].

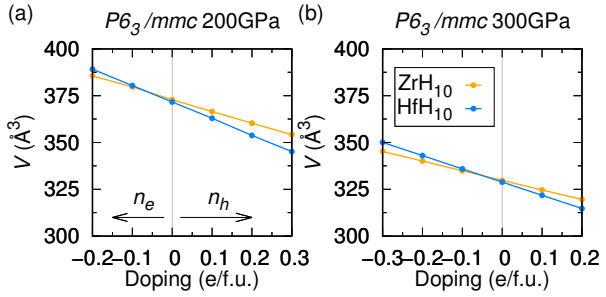

FIG. 2. The unit cell volumes of $P6_3/mmc$ ZrH_{10} and HfH_{10} as a function of doping concentration at different pressures.

Unlike the clathrate structure of face-centered cubic LaH_{10}, planar penta-graphene-like ZrH_{10} and HfH_{10} pos-

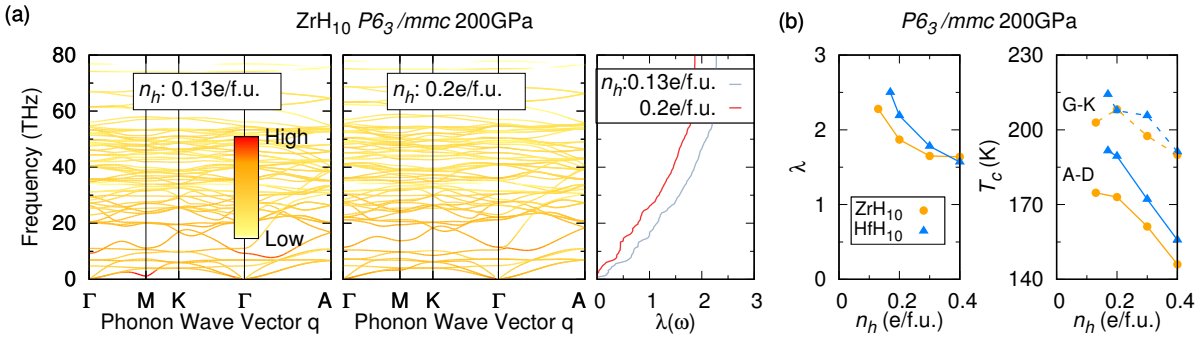

FIG. 3. (a) The distributions of the EPC strength and the integrated electron-phonon coefficients of $P6_3/mmc$ ZrH_{10} under different hole doping concentrations at 200 GPa. The color code is determined by the strength of EPC. (b) The integrated electron-phonon coefficients and the superconducting transition temperatures of hole doped $P6_3/mmc$ ZrH_{10} and HfH_{10} at 200 GPa.

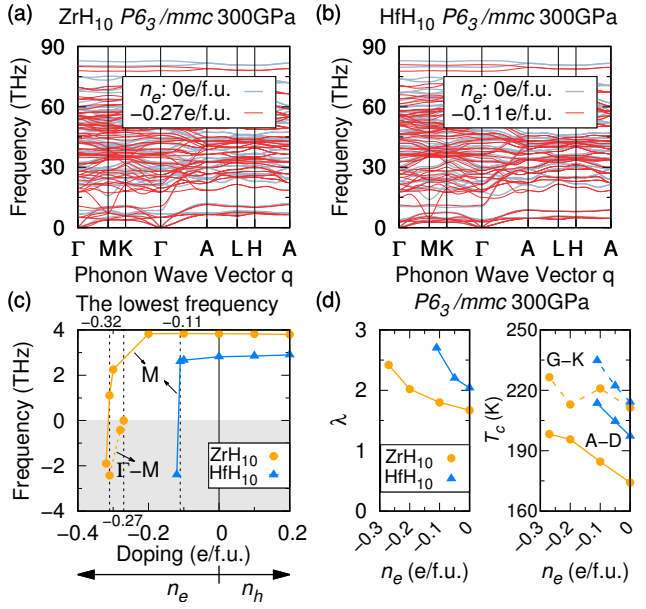

FIG. 4. Phonon dispersions of $P6_3/mmc$ ZrH_{10} (a) and HfH_{10} (b) at 300 GPa under different electron doping concentrations. (c) Evolution of the lowest phonon frequency at M point and along Γ-M as a function of doping concentration at 300 GPa. (d) The integrated electron-phonon coefficients and the superconducting transition temperatures of electron-doped $P6_3/mmc$ ZrH_{10} and HfH_{10} at 300 GPa.

sess a hexagonal structure in a space group of $P6_3/mmc$ (see Fig. 1(a)). Based on this hexagonal structure, the influence of electron and hole dopings under pressures has been studied. At 200 GPa, large imaginary frequencies (especially in the vicinity of M high symmetry point) can be observed in the phonon dispersion of the undoped $P6_3/mmc$ ZrH_{10} and HfH_{10} in Fig. 1(b-c), indicating that they are dynamically unstable at this pressure. The imaginary phonon frequencies in ZrH_{10} arise from the acoustic modes near M point while those in HfH_{10} are mainly contributed by optical branches near M and Γ points. To investigate the doping effects on the vibrational stability, the changes of the lowest phonon frequency at M point for ZrH_{10} and HfH_{10} are shown in Fig. 1(d). It is seen that the phonon mode with imaginary frequency at M point further softens as electron doping concentration increases. On the contrary, it gradually hardens as hole doping concentration increases. The imaginary phonon frequencies at M point are completely eliminated at hole doping concentrations of 0.13 e/f.u. and 0.09 e/f.u. for ZrH_{10} and HfH_{10}, respectively. However, the imaginary phonon frequencies along Γ-A path in HfH_{10} still exist until the hole doping concentration is above approximately 0.17 e/f.u.. Similar doping effects are also observed in the clathrate FCC phase of ZrH_{10} and HfH_{10} (see Fig. S1 in the Supporting Information), where imaginary phonon frequencies at X point can be eliminated by hole doping. Moreover, the influence of hole (electron) doping on the volume of the unit cell is analogous to that of exerting a hydrostatic (negative) pressure. As shown in Fig. 2, hole doping is conducive to reducing the volumes of the $P6_3/mmc$ phase, which is similar to the effects of exerting a higher hydrostatic pressure. Therefore, suitable hole doping helps to eliminate the imaginary phonon frequencies and stabilize the phase at a lower pressure of 200 GPa. In the contrast, cell volume expands as electron doping concentration increases, which is similar to exerting a negative pressure on the $P6_3/mmc$ phase. Thus, electron doping is detrimental to the dynamical stability of ZrH_{10} and HfH_{10} at 300 GPa.

To study the superconductivity of hole-doped $P6_3/mmc$ ZrH_{10} and HfH_{10} at 200 GPa, the EPC strength, the integrated electron-phonon coefficient, electronic DOS, and T_c under different hole doping concentrations are investigated. As presented in Fig. 3(a), phonons in the low frequency region ($\leq$ 20 THz) possess higher EPC strength. One striking feature of phonon dispersion is the presence of extremely soft phonon modes at M point at n_h =0.13 e/f.u., where the high EPC strength arises from the large phonon line widths and the low frequencies of the soft modes. By further

increasing hole doping concentration, the soft mode at M point hardens, and the EPC strength decreases. The integrated EPC parameter $\lambda(\omega)$ climbs less rapidly in the low-frequency range with the increase of hole doping concentration, leading to a smaller total EPC parameter and T_c (see Fig. 3(b)): approximately 28.1% decrease in λ and 16.4% (6.4%) decrease in T_c^{A-D} (T_c^{G-K}) from n_h=0.13 e/f.u. to n_h=0.4 e/f.u. in ZrH_{10} at 200 GPa. It is also noted that the monotonically decreased λ and T_c as n_h increases are different from the changes of DOS at E_F (see FIG. S2 (a) in the Supporting Information), which increases first and then decreases. Similar results are also found for HfH_{10}. However, the maximum EPC strength in HfH_{10} is attained between Γ-A path (see Fig. S3 in the Supporting Information) instead of at M point. The maximum λ (2.50) and T_c (191.6 K and 214.2 K from A-D and G-K methods, respectively) are reached at a hole doping concentration of 0.17 e/f.u. in HfH_{10}.

It is seen from Fig. 4(a-b) that, at 300 GPa, both $P6_3/mmc$ ZrH_{10} and HfH_{10} are lattice dynamically stable, which are consistent with previous report[21]. With electron doping, phonons are prone to be softened, leading to potential lattice instability. As depicted in Fig. 4(c), the lowest phonon frequencies at M point remain nearly unchanged under low electron or hole doping concentrations, whereas they drop drastically with increasing electron doping concentration. The lattice dynamical instabilities appear at electron doping concentrations greater than -0.27 e/f.u. and -0.11 e/f.u. for ZrH_{10} and HfH_{10}, respectively. Stronger EPC is induced by the greatly softened optical branches after electron doping near M point (see Fig. S4 and S5 in the Supporting Information). Consequently, $\lambda(\omega)$ in electron-doped systems boosts more remarkably at the low-frequency range compared to the pristine systems, resulting in enhancements of λ and T_c in both ZrH_{10} and HfH_{10} (see Fig. 4 (d)).

In conclusion, the doping effects on the lattice dynamical stability and superconductivity of penta-graphene-like ZrH_{10} and HfH_{10} have been studied from first-principles calculations. Hole doping is found to be beneficial to the lattice dynamical stability of $P6_3/mmc$ ZrH_{10} and HfH_{10}, leading to a reduction of the stabilization pressure. In the meantime, the strong EPC induced by hole doping preserves exceptional superconductivity at lower pressures. At higher pressure, where the structures are found to be dynamically stable, electron doping can soften the phonon modes, leading to an increased EPC parameter and therefore T_c.

ACKNOWLEDGMENTS

This work is supported by the Zhejiang Provincial Natural Science Foundation (LR19A040001), the National Natural Science Foundation of China (11874313), and the Research Grants Council of Hong Kong (17201019 and 17306721). The authors are grateful for the research computing facilities offered by ITS, HKU.

* yuechen@hku.hk

[1] A. M. Shipley, M. J. Hutcheon, R. J. Needs, and C. J. Pickard, Phys. Rev. B **104**, 054501 (2021).
[2] L. Boeri and G. B. Bachelet, J. Phys. Condens. Matter **31**, 234002 (2019).
[3] N. W. Ashcroft, Phys. Rev. Lett. **21**, 1748 (1968).
[4] M. Eremets and I. Troyan, Nat. Mater. **10**, 927 (2011).
[5] J. A. Flores-Livas, L. Boeri, A. Sanna, G. Profeta, R. Arita, and M. Eremets, Phys. Rep. **856**, 1 (2020).
[6] T. Bi, N. Zarifi, T. Terpstra, and E. Zurek, in *Reference Module in Chemistry, Molecular Sciences and Chemical Engineering* (Elsevier, 2019).
[7] Y. Quan, S. S. Ghosh, and W. E. Pickett, Phys. Rev. B **100**, 184505 (2019).
[8] L. Gao, Y. Y. Xue, F. Chen, Q. Xiong, R. L. Meng, D. Ramirez, C. W. Chu, J. H. Eggert, and H. K. Mao, Phys. Rev. B **50**, 4260 (1994).
[9] H. Wang, J. S. Tse, K. Tanaka, T. Iitaka, and Y. Ma, Proc. Natl. Acad. Sci. U.S.A. **109**, 6463 (2012).
[10] Z. Shao, D. Duan, Y. Ma, H. Yu, H. Song, H. Xie, D. Li, F. Tian, B. Liu, and T. Cui, Inorg. Chem. **58**, 2558 (2019).
[11] L. Ma, K. Wang, Y. Xie, X. Yang, Y. Wang, M. Zhou, H. Liu, X. Yu, Y. Zhao, H. Wang, G. Liu, and Y. Ma, "High-tc superconductivity in clathrate calcium hydride CaH6," (2021), arXiv:2103.16282 [cond-mat.supr-con].
[12] F. Peng, Y. Sun, C. J. Pickard, R. J. Needs, Q. Wu, and Y. Ma, Phys. Rev. Lett. **119**, 107001 (2017).
[13] I. A. Troyan, D. V. Semenok, A. G. Kvashnin, A. V. Sadakov, O. A. Sobolevskiy, V. M. Pudalov, A. G. Ivanova, V. B. Prakapenka, E. Greenberg, A. G. Gavriliuk, I. S. Lyubutin, V. V. Struzhkin, A. Bergara, I. Errea, R. Bianco, M. Calandra, F. Mauri, L. Monacelli, R. Akashi, and A. R. Oganov, Adv. Mater. **33**, 2006832 (2021).
[14] C. Heil, S. di Cataldo, G. B. Bachelet, and L. Boeri, Phys. Rev. B **99**, 220502 (2019).
[15] P. Kong, V. S. Minkov, M. A. Kuzovnikov, A. P. Drozdov, S. P. Besedin, S. Mozaffari, L. Balicas, F. F. Balakirev, V. B. Prakapenka, S. Chariton, D. A. Knyazev, E. Greenberg, and M. I. Eremets, Nat. Commun. **12**, 1 (2021).
[16] N. P. Salke, M. M. D. Esfahani, Y. Zhang, I. A. Kruglov, J. Zhou, Y. Wang, E. Greenberg, V. B. Prakapenka, J. Liu, A. R. Oganov, and J.-F. Lin, Nat. Commun. **10**, 1 (2019).
[17] D. V. Semenok, A. G. Kvashnin, A. G. Ivanova, V. Svitlyk, V. Y. Fominski, A. V. Sadakov, O. A. Sobolevskiy, V. M. Pudalov, I. A. Troyan, and A. R. Oganov, Mater. Today **33**, 36 (2020).
[18] H. Liu, I. I. Naumov, R. Hoffmann, N. W. Ashcroft, and R. J. Hemley, Proc. Natl. Acad. Sci. U.S.A. **114**, 6990 (2017).
[19] A. Drozdov, P. Kong, V. Minkov, S. Besedin, M. Kuzovnikov, S. Mozaffari, L. Balicas, F. Balakirev, D. Graf, V. Prakapenka, E. Greenberg, D. A. Knyazev, M. Tkacz,

and M. I. Eremets, Nature **569**, 528 (2019).
[20] I. A. Kruglov, D. V. Semenok, H. Song, R. Szczesniak, I. A. Wrona, R. Akashi, M. M. Davari Esfahani, D. Duan, T. Cui, A. G. Kvashnin, and A. R. Oganov, Phys. Rev. B **101**, 024508 (2020).
[21] H. Xie, Y. Yao, X. Feng, D. Duan, H. Song, Z. Zhang, S. Jiang, S. A. T. Redfern, V. Z. Kresin, C. J. Pickard, and T. Cui, Phys. Rev. Lett. **125**, 217001 (2020).
[22] D. V. Semenok, I. A. Kruglov, I. A. Savkin, A. G. Kvashnin, and A. R. Oganov, Curr. Opin. Solid State Mater. Sci. **24**, 100808 (2020).
[23] A. Drozdov, M. Eremets, I. Troyan, V. Ksenofontov, and S. I. Shylin, Nature **525**, 73 (2015).
[24] M. Einaga, M. Sakata, T. Ishikawa, K. Shimizu, M. I. Eremets, A. P. Drozdov, I. A. Troyan, N. Hirao, and Y. Ohishi, Nat. Phys. **12**, 835 (2016).
[25] E. Snider, N. Dasenbrock-Gammon, R. McBride, M. Debessai, H. Vindana, K. Vencatasamy, K. V. Lawler, A. Salamat, and R. P. Dias, Nature **586**, 373 (2020).
[26] J. G. Bednorz and K. A. Müller, Z. Phys., B Condens. Matter **64**, 189 (1986).
[27] B. Keimer, S. A. Kivelson, M. R. Norman, S. Uchida, and J. Zaanen, Nature **518**, 179 (2015).
[28] A. Iyo, K. Kawashima, S. Ishida, H. Fujihisa, Y. Gotoh, H. Eisaki, and Y. Yoshida, J. Am. Chem. Soc. **140**, 369 (2018).
[29] S. Villa-Cortes and O. De la Pena-Seaman, J. Phys. Condens. Matter **33**, 425401 (2021).
[30] J. Bardeen, L. N. Cooper, and J. R. Schrieffer, Phys. Rev. **108**, 1175 (1957).
[31] Y. Sun, J. Lv, Y. Xie, H. Liu, and Y. Ma, Phys. Rev. Lett. **123**, 097001 (2019).
[32] C. Wang, S. Yi, S. Liu, and J.-H. Cho, Phys. Rev. B **102**, 184509 (2020).
[33] C. Wang, S. Liu, H. Jeon, S. Yi, Y. Bang, and J.-H. Cho, Phys. Rev. B **104**, L020504 (2021).
[34] Y. Ge, F. Zhang, R. P. Dias, R. J. Hemley, and Y. Yao, Mater. Today Phys. **15**, 100330 (2020).
[35] P. Giannozzi, S. Baroni, N. Bonini, M. Calandra, R. Car, C. Cavazzoni, D. Ceresoli, G. L. Chiarotti, M. Cococcioni, I. Dabo, A. D. Corso, S. de Gironcoli, S. Fabris, G. Fratesi, R. Gebauer, U. Gerstmann, C. Gougoussis, A. Kokalj, M. Lazzeri, L. Martin-Samos, N. Marzari, F. Mauri, R. Mazzarello, S. Paolini, A. Pasquarello, L. Paulatto, C. Sbraccia, S. Scandolo, G. Sclauzero, A. P. Seitsonen, A. Smogunov, P. Umari, and R. M. Wentzcovitch, J. Phys. Condens. Matter **21**, 395502 (2009).
[36] P. Giannozzi, O. Andreussi, T. Brumme, O. Bunau, M. B. Nardelli, M. Calandra, R. Car, C. Cavazzoni, D. Ceresoli, M. Cococcioni, N. Colonna, I. Carnimeo, A. D. Corso, S. de Gironcoli, P. Delugas, R. A. DiStasio, A. Ferretti, A. Floris, G. Fratesi, G. Fugallo, R. Gebauer, U. Gerstmann, F. Giustino, T. Gorni, J. Jia, M. Kawamura, H.-Y. Ko, A. Kokalj, E. Küçükbenli, M. Lazzeri, M. Marsili, N. Marzari, F. Mauri, N. L. Nguyen, H.-V. Nguyen, A. O. de-la Roza, L. Paulatto, S. Poncé, D. Rocca, R. Sabatini, B. Santra, M. Schlipf, A. P. Seitsonen, A. Smogunov, I. Timrov, T. Thonhauser, P. Umari, N. Vast, X. Wu, and S. Baroni, J. Phys. Condens. Matter **29**, 465901 (2017).
[37] W. Kohn and L. J. Sham, Phys. Rev. **140**, A1133 (1965).
[38] S. Baroni, S. De Gironcoli, A. Dal Corso, and P. Giannozzi, Rev. Mod. Phys. **73**, 515 (2001).
[39] D. R. Hamann, Phys. Rev. B **88**, 085117 (2013).
[40] M. Schlipf and F. Gygi, Comput. Phys. Commun. **196**, 36 (2015).
[41] J. P. Perdew, K. Burke, and M. Ernzerhof, Phys. Rev. Lett. **77**, 3865 (1996).
[42] G. Kresse and J. Furthmüller, Comput. Mater. Sci. **6**, 15 (1996).
[43] W. Tang, E. Sanville, and G. Henkelman, J. Phys. Condens. Matter **21**, 084204 (2009).
[44] M. Wierzbowska, S. de Gironcoli, and P. Giannozzi, "Origins of low- and high-pressure discontinuities of T_c in niobium," (2006), arXiv:0504077 [cond-mat.supr-con].
[45] P. B. Allen and R. C. Dynes, Phys. Rev. B **12**, 905 (1975).
[46] L. P. Gorkov and V. Z. Kresin, Rev. Mod. Phys. **90**, 011001 (2018).
[47] C. Wang, S. Yi, and J.-H. Cho, Phys. Rev. B **101**, 104506 (2020).